ea engenharia agrícola

Journal of the Brazilian Association of Agricultural Engineering
ISSN: 1809-4430 (on-line)

GEOMETRY AND HEAD LOSS IN VENTURI INJECTORS THROUGH COMPUTATIONAL FLUID DYNAMICS[1]

Doi:http://dx.doi.org/10.1590/1809-4430-Eng.Agric.v36n3p482-491/2016

JUAN MANZANO[2], CARMEN V. PALAU[3], BENITO M. DE AZEVEDO[4], GUILHERME V. DO BOMFIM[5], DENISE V. VASCONCELOS[6]

ABSTRACT: To determine the influence of geometry on the hydrodynamic behavior of Venturi injectors, using computational fluid dynamics techniques, we studied, at the *Universitat Politècnica de València*, Valencia, Spain, the geometric parameters that exert the most influence on head losses: the relationship between throat diameter and nozzle (β), nozzle angle (α_1) and diffuser angle (α_2). In addition, three throat morphologies (B1: nozzle-throat and throat-diffuser with a sharp edge; B2: nozzle-diffuser with a zero-length, sharp-edge throat; B3: nozzle-throat and throat-diffuser with rounded edge). We analyzed their influence on the velocity distribution and differential pressure between inlet and throat (DP/γ), throat and outlet ($\Delta h_v/\gamma$), and outlet and throat ($(P_3-P_2)/\gamma$). The development of the velocity profile from the throat is slower the greater β is and the lower α_2 is. DP/γ decreases with β, increases with α_1 and varies little with α_2. $\Delta h_v/\gamma$ decreases with β and increases with α_1 and α_2. $(P_3-P_2)/\gamma$ decreases with β and increases with α_1 and α_2. Geometry B3 decreases the losses and delays the onset of cavitation. Thus, the lower β and the higher α_2, the greater the losses; however, the influence of α_1 is less clear. The rounded edges produce lower head losses.

KEY WORDS: Chemigation. Fertirrigation. DFC.

GEOMETRÍA Y PÉRDIDAS DE CARGA EN INYECTORES VENTURI MEDIANTE LA DINÁMICA DE FLUIDOS COMPUTACIONAL[1]

RESUMEN: Para determinar la influencia de la geometría en el comportamiento hidrodinámico de inyectores Venturi, mediante técnicas de dinámica de fluidos computacional, se estudió, en la *Universitat Politècnica de València*, Valencia, España, los parámetros geométricos que más influencian las pérdidas de carga: relación entre diámetro de la garganta y tobera (β), ángulo de la tobera (α_1) y ángulo del difusor (α_2). Además, tres morfologías de la garganta (B1: tobera-garganta y garganta-difusor en arista viva; B2: tobera-difusor con garganta de longitud nula y en arista viva; B3: tobera-garganta y garganta-difusor en arista redondeadas). Se ha analizado su influencia en la distribución de velocidad y en la presión diferencial entre entrada y garganta (DP/γ), garganta y salida ($\Delta h_v/\gamma$), y salida y garganta ($(P_3-P_2)/\gamma$). El desarrollo del perfil de velocidades a partir de la garganta es más lento cuanto mayor es β y menor es α_2. DP/γ disminuye con β, aumenta con α_1 y es poco variable con α_2. $\Delta h_v/\gamma$ disminuye con β y aumenta con α_1 y α_2. $(P_3-P_2)/\gamma$ disminuye con β y α_1, y aumenta con y α_2. La geometría B3 disminuye las pérdidas y retarda la aparición de la cavitación. Así, cuanto menor es β y cuanto mayor es α_2, mayores son las pérdidas de carga, sin embargo, la influencia de α_1 no es tan clara. Las aristas redondeadas producen menores perdidas de carga.

PALABRAS-CLAVE: quimigación, fertirigación, DFC.

[1] Parte da tese de Doutorado feita na Universitat Politècnica de València, Valência, Espanha.

[2] Engº Agrônomo, Prof. Doutor, Departamento de Ingeniería Rural y Agroalimentaria, UPV/Valencia-España, Fone: (+34) 963877540, juamanju@agf.upv.es
[3] Engª Agrônoma, Prof. Doutor, Departamento de Ingeniería Rural y Agroalimentaria, UPV/Valencia-España, virpaes@agf.upv.es
[4] Engº Agrônomo, Prof. Doutor, Departamento de Engenharia Agrícola, UFC/Fortaleza-CE, benitoazevedo@hotmail.com
[5] Engº Agrônomo, Pesq. Doutor, Departamento de Engenharia Agrícola, UFC/Fortaleza-CE, guile2007@gmail.com
[6] Engª Agrônoma, Pesq. Doutor, Departamento de Engenharia Agrícola, UFC/Fortaleza-CE, denisevasconcelos@hotmail.com

Recebido pelo Conselho Editorial em: 26/08/2014
Aprovado pelo Conselho Editorial em: 07/03/2016

INTRODUCTION

The contribution of chemicals in the water, referred to as chemigation, is a technique that is currently often developed in pressurized irrigation methods (SANTOS et al., 2012) such as a sprinkling (DANTAS NET et al., 2013) and localized irrigation (REZENDE et al, 2010;. URIBE et al, 2013).

An injection device that is often used in chemigation, in small and medium agronomic crops, is the Venturi nozzle (DIMITRIOS et al., 2014). It is an economical, robust hydraulically operated system, without requiring external energy input (SANTOS et al., 2012). Nevertheless, the high head losses caused by its operation (SUN & NIU, 2012) correspond to the least 30% of the inlet pressure (ARVIZA, 2001). It may also present problems regarding regulation, air injection, or cavitation (MANZANO, 2008).

The Venturi injector consists of three parts – a convergent section (nozzle), followed a constant section (throat), ending in a gradual expansion (diffuser) (Figure 1). The geometric variables defining the injector are the relationship of diameters $\beta=D_2/D_1$, the nozzle angle (α_1), and the diffuser angle (α_2) (MANZANO, 2008).

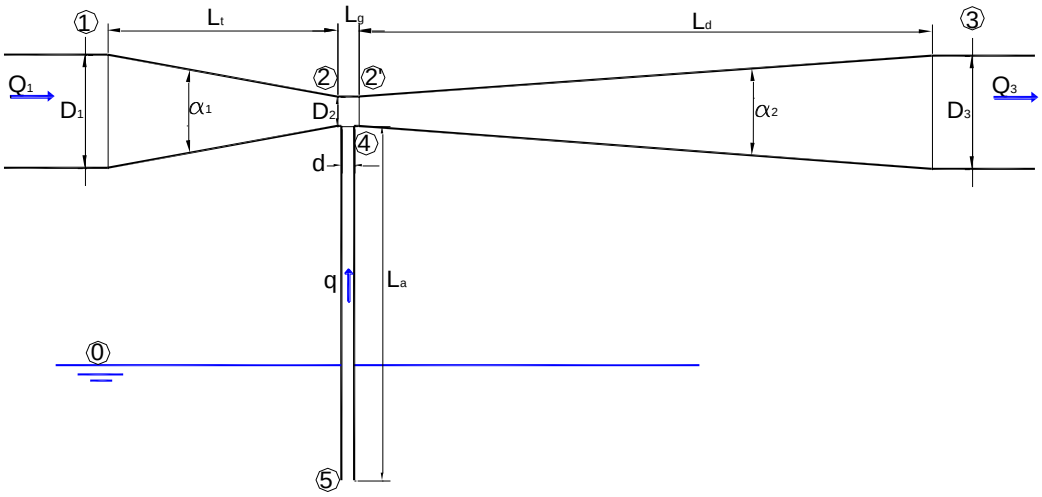

FIGURE 1. Venturi nozzle diagram, Valencia, *Universitat Politècnica de València*, 2008. Q_1: inflow; q: injected flow; Q_3: outflow; D_1: nozzle diameter; d: suction diameter; D_2: throat diameter; D_3: diffuser diameter; L_t: nozzle length; L_g: throat length; L_a: suction length; L_d: diffuser length; α_1: nozzle angle; α_2: diffuser angle. Sections: 0: free solution for injection; 1: Venturi inlet; 2: Venturi throat; 3: Venturi outlet; 4: suction outlet; 5: suction inlet.

Venturi-type injectors initially based their characteristics on flowmeters based on the same hydraulic effect, where certain angle values are recommended for the throat ($\alpha_1 = 21°\pm1$, $7° \leq \alpha_2 \leq 15°$), enabling production of minimum losses (INTERNATIONAL ORGANIZATION FOR STANDARDIZATION, 2003). Nevertheless, in commercial equipment, these angles are greater, in particular α_1. This angular increase is associated with reduced length (cost reduction), although there is an increase in losses. Commercial values for the relationship of diameters (β) range between 0.12 and 0.5. For the nozzle angle (α_1), commercial values range between 10° and 75°. Regarding the diffuser angle (α_2), commercial values range between 5 and 31 (MANZANO, 2008).

Other important geometrical characteristics are the junctions of the nozzle with the throat and the diffuser, which may affect the total head loss and risk of cavitation. The International Organization for Standardization (2003) establishes a throat length (L_g) of $D_2\pm0.03$ D_2 and, depending on the construction material, recommends the rounding of edges. The throat length given by commercial manufacturers varies greatly and junctions frequently have sharp edges.

The computational fluid dynamics (CFD) techniques provide numerical solutions for problems in fluid mechanics with the aid of computers (BAYLAR et al., 2009; WENDT, 2009). This technique is widely used in Hydraulic Engineering, following the example of fertilizer injection systems (YEOH et al., 2012), showing the effect of geometry to obtain the values of the system characteristic variables.

In summary, the phases of a CFD method consist of preprocessing (problem definition), processing (solution) and post-processing (analysis of results). The preprocessing phase defines the specific geometry of the system being simulated, discretizing the computational domain with the mesh generation. The following are defined: physical aspects of the problem; governing equations and models for processes taking place in the system; chemical reactions; and initial and boundary conditions. Finally, numerical calculation parameters should be established. The processing phase consists of approximating the unknown variables by simple functions and their replacement in the governing equations. The post-processing phase defines the analysis of the results through a graphical representation (MANZANO, 2008).

The results developed by the CFD techniques are approximate values of the behavior of the thermodynamic variables. When theoretical models for checking the accuracy of these values are not available, experimental tests are required (LODOÑO et al., 2004). Therefore, the suitability of CFD techniques to describe the hydraulic behavior of Venturi injectors has been proven by MANZANO & PALAU (2005), as the experimental results and those obtained by computer were very similar.

In this paper, we employed CFD techniques to analyze the geometric parameters that characterize the Venturi injector and have the greatest impact on the head loss. We thus intended to determine their influence on the hydrodynamic behavior of the element. As an associated objective, we refined the computational calculation methodology, which has proven to be an effective tool for improving elements and devices in agricultural hydraulic applications.

MATERIAL AND METHODS

The test was conducted in the Hydraulics and Localized Irrigation Laboratory of the Department of Rural and Agrifood Engineering of the *Universitat Politècnica de València*, Valencia, Spain (39°29'N, 0°23'20"W).

The CFD techniques were used to study five different levels of the relationship of diameters (β) (0.1; 0.2; 0.3; 0.4; 0.5), nozzle angle (α_1) (7°; 15°; 21º; 40º; 60º), and diffuser angle (α_2) (5°; 7°; 15°; 30°; 60°), for a total of 13 models with different geometries. For all injectors considered, we assumed a nominal diameter (DN_1) of 63 mm and a total length (L_t) of 775 mm, with the thirteen combinations (Table 1).

TABLE 1. Structural parameters for Venturi nozzle models, *Universitat Politècnica de València*, 2008.

Geometries/Models	A1	A2	A3	A4	A5	A6	A7	A8	A9	A10	A11	A12	A13
β	0.1	0.2	0.3	0.4	0.5	0.3	0.3	0.3	0.3	0.3	0.3	0.3	0.3
α_1	21	21	21	21	21	21	21	21	21	7	15	40	60
α_2	7	7	7	7	7	5	15	30	60	7	7	7	7

β: relationship of diameters; α_1: converging nozzle angle; α_2: diverging diffuser angle.

We also employed the CFD techniques to study the injector operation for three throat morphologies (Figure 2). The first morphology represents the nozzle-throat and throat-diffuser junctions with a sharp edge (B1). The second shows the nozzle-diffuser junction throat with zero length and a sharp edge (B2). The third shows the nozzle-throat and throat-diffuser junctions with a rounded edge (B3).

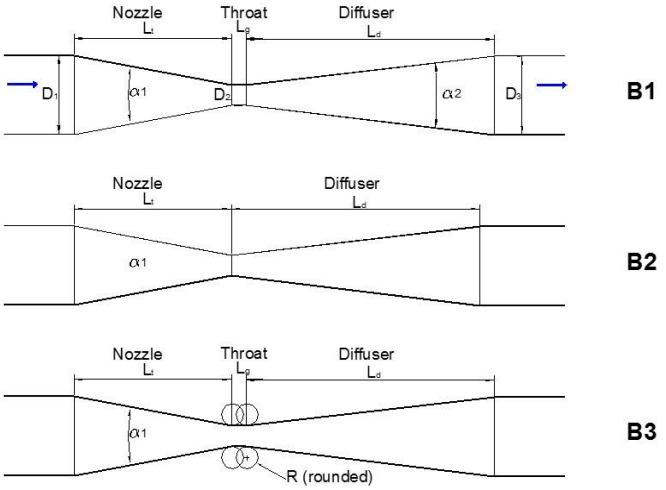

FIGURE 2. Diagrams of the three compared throat geometries of the Venturi nozzle, Valencia, *Universitat Politècnica de València*, 2008. B1: nozzle-throat and throat-diffuser junctions with a sharp edge; B2: nozzle-diffuser junction with zero length and a sharp edge; B3: nozzle-throat and throat-diffuser junctions with a rounded edge.

The software used for the application of CFD were GAMBIT.2.2.30 (preprocessing), FLUENT.6.2.16 (processed) and TECPLOT.360 (post-processing).

GAMBIT has been employed in the construction of the geometry and meshing (Figure 3A). The mesh was decomposed into different subdomains, combining meshes in structured tetrahedral and prismatic structures. The size of each cell is between 0.3 mm^3 and 0.2 mm^3 and the total number of cells was greater than 5 10^5. We tested different mesh sizes by comparing the results obtained with each of them. The mesh was built in a structured (hexahedral) way, according the main direction of the flow throughout the domain, except in areas of pipe connection (not allowed by the software). In these cases, we intercalated unstructured (tetrahedral) meshes, resulting in a hybrid meshing type (Figure 3B). Near the walls of the Venturi, the mesh was refined for better resolution of the boundary layer (Figure 3C). All geometries were modeled in three dimensions, reproducing as accurately as possible the internal dimensions of the tested prototypes (Figure 3D). The Cartesian coordinate system was used, and we defined the origin at the point of confluence of the Venturi axis and the suction axis.

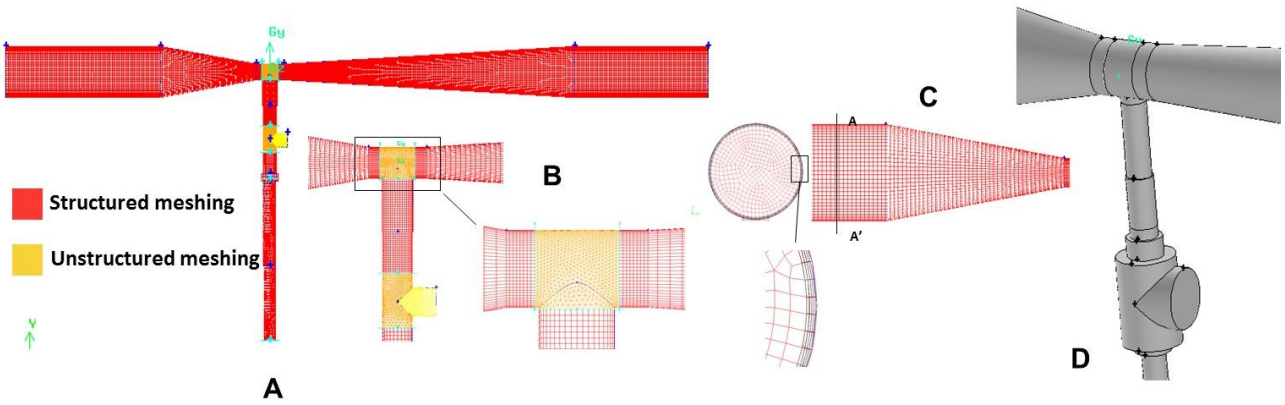

FIGURE 3. Diagram of the geometry of a Venturi injector (A), detail of the structured and unstructured areas (B), detail of the boundary layer (C), and example of meshing of model A3 (D), Valencia, *Universitat Politècnica de València*, 2008.

FLUENT was used to define the Solver, performing the analysis with three dimensions and double precision. After the definition, we imported the mesh generated by GAMBIT, checking it for connectivity and scaling. As boundary conditions, we set the pressure in the outlet section (15 m.c.a.) and the average inlet speed of the Venturi (1.5 m s^{-1}), considering null the injection flow.

The Solver formulation selection was performed through the governing equations of continuity and momentum (VASATA et al., 2011). The selection of the mathematical model for the formulation was made considering the turbulent flow, being added to the above governing equations. The Reynolds-Averaged Navier-Stokes (RANS) equation model – currently one two most widely used (CHAN et al., 2014; SANDERS et al., 2011) – was employed. In the RANS model, we employed the Reynolds Stress Model (RSM) (ALPTEKIN et al., 2014), with standard functions for the wall treatment, selecting as the basis for the calculation the turbulence intensity (5%) and the hydraulic diameter of the upstream flow in the inlet and outlet sections of the Venturi injector. The equations above were discretized using the finite volume method (FVM) (MELLADO et al., 2013), using the Tridiagonal Matrix Algorithm (TDMA) (AL-HASSAN, 2005) with a sequential (segregated) resolution.

TECPLOT was used to define the graphical representation of all calculated, scalar or vector variables. Each model provided complete graphical and numerical information.

Thus, first, we modeled the operation of the injector for variables β, α_1 and α_2 while maintaining constant the Venturi injector nozzle diameter and length. With the resulting quantitative data, we determined the speed distribution and the influence of each geometric variable in DP/γ, $\Delta h_v/\gamma$, and $(P_3-P_2)/\gamma$. The DP/γ variable is the differential pressure between the inlet and throat ($(P_1-P_2)/\gamma$); $\Delta h_v/\gamma$ are total losses in the injector or the pressure difference between the throat and the outlet ($(P_1-P_3)/\gamma$); and $(P_3-P_2)/\gamma$ is the pressure difference between the outlet and the throat. The weight of variables β, α_1 and α_2 in DP/γ, $\Delta h_v/\gamma$ and $(P_3-P_2)/\gamma$, from the quantitative data obtained with the CFD was obtained with the analysis of variance and multiple regression (1% probability, F test), through the Statgraphics Plus 5.1 software application.

Second, for the same boundary conditions, we obtained the pressure and speed distribution in a vertically symmetrical plane in the throat. The pressures analyzed were P_1/γ (injector inlet), P_2/γ (suction point), P_3/γ (injector outlet), DP/γ (P_1/γ - P_2/γ), $\Delta h_v/\gamma$ (P_3/γ - P_2/γ) and P_{min}/γ (pressure at the lowest analyzed volume, which is obtained at the wall in all cases).

RESULTS AND DISCUSSION

Figures 4, 5 and 6 show the velocity distributions and DP/γ, $\Delta h_v/\gamma$ and $(P_3-P_2)/\gamma$ as a function of β, α_1, and α_2.

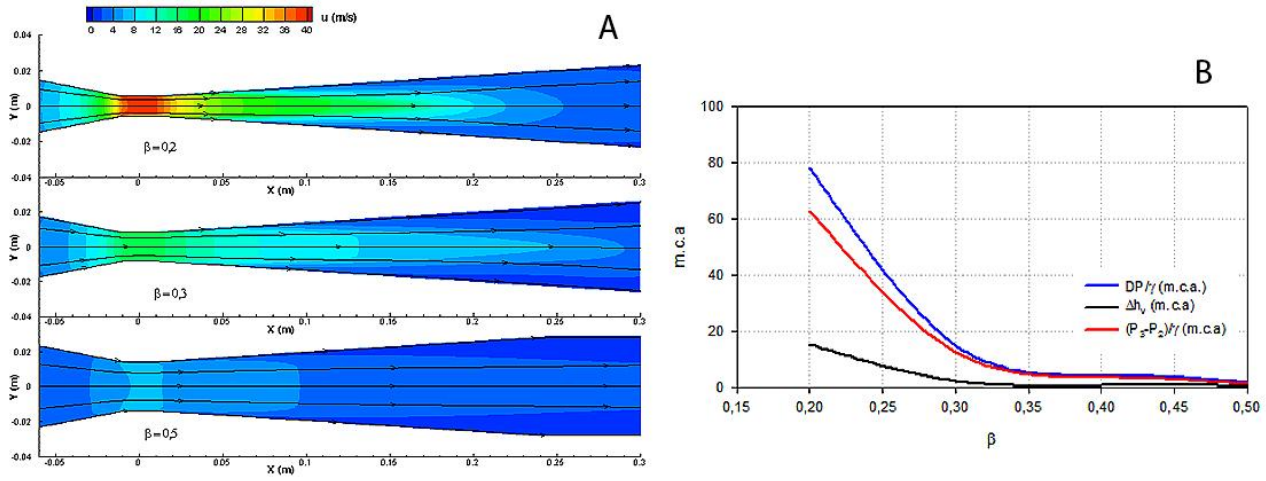

FIGURE 4. Speed distributions (A) and DP/γ, $\Delta h_v/\gamma$ y $(P_3-P_2)/\gamma$ (B) for different values of β (fixed angles), Valencia, *Universitat Politècnica de València*, 2008.

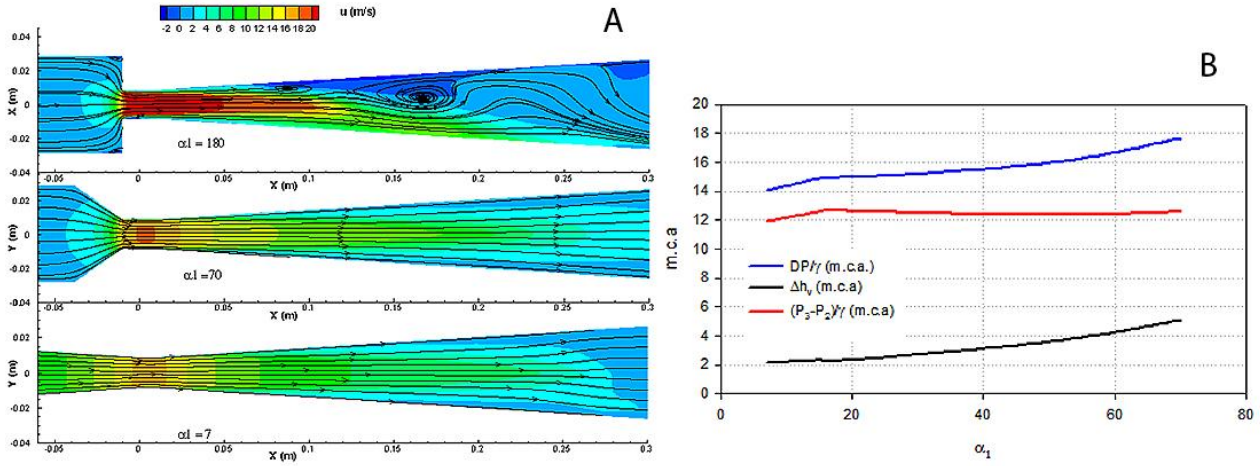

FIGURE 5. Speed distributions (A) and DP/γ, $\Delta h_v/\gamma$ and $(P_3-P_2)/\gamma$ (B) for different values of α_1 (fixed angles), Valencia, *Universitat Politècnica de València*, 2008.

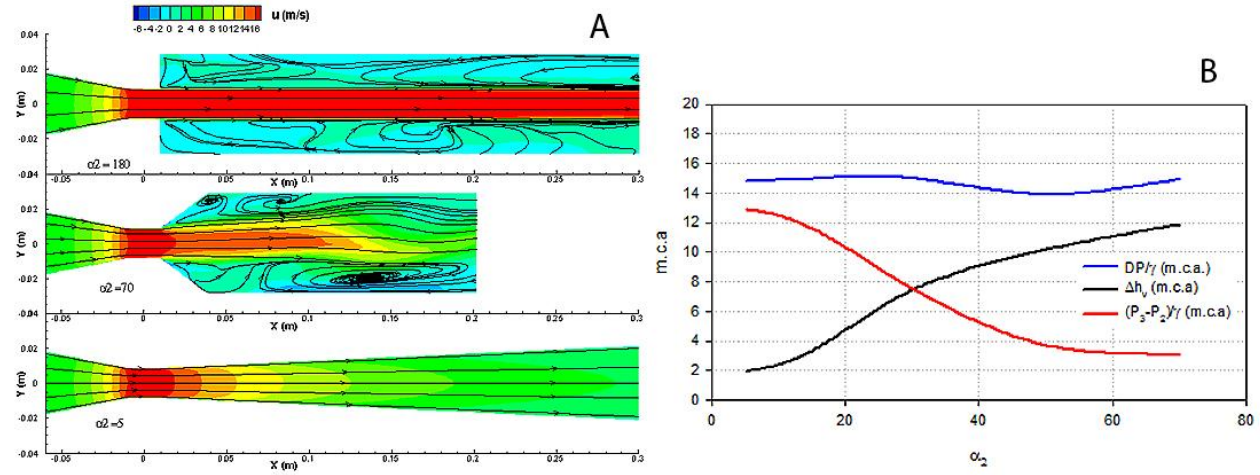

FIGURE 6. Speed distributions (A) and DP/γ, $\Delta h_v/\gamma$ and $(P_3-P_2)/\gamma$ (B) for different values of α_2 (fixed angles), Valencia, *Universitat Politècnica de València*, 2008.

The results obtained with the CFD techniques were as expected according to hydrodynamics. The development of the speed profile from the throat is slower as β increases and α_2 decreases. A more gradual convergence decreases flow disturbances. DP/γ decreases with β, increases with α_1 and varies little with α_2 with a minimum of 50°. $\Delta h_v/\gamma$ losses decrease with β and increase with α_1 and α_2. $(P_3-P_2)/\gamma$ decreases with β and α_1, increasing with α_2.

With the results, we can see that the pressure loss relates to the geometry of the injector. We can see that the lower the relationship of diameters, the greater the loss. For the diffuser angle, we also note a clear trend of increasing losses with the angle. Nevertheless, the influence of the nozzle angle is not so clear.

The following statistical analyses indicate, based on quantitative data obtained with the CFD, the weight of variables β, α_1 and α_2 in DP/γ, $\Delta h_v/\gamma$ and $(P_3-P_2)/\gamma$ (Tables 2, 3 and 4).

TABLE 2. Analysis of variance and multiple regression for DP/γ, Valencia, *Universitat Politècnica de València*, 2008.

Source	GL	Sum of squares	Mean square	F-Quotient	P-Value
Model	3	6.17218	2.05739	179.04	0,0000**
Residue	12	0.137897	0.0114914	-	-
Total	15	6.31008	-	-	-
Parameter		Estimate	Standard error	T-Statistic	P-Value
Constant		0.353347	0.227437	1.5536	0.1462ns
log (a1)		0.0493619	0.0391969	1.25933	0.2319ns
log (a2)		-0.145939	0.0263635	-5.53563	0.0001**
log (b)		-3.46304	0.152485	-22.7108	0.0000**

**Significant to 1%; R^2 adjusted from 97.26%; standard error of 0.11; mean absolute error of 0.07; Durbin-Watson test of 1.44 (P=0.03); Lag_l residual autocorrelation of 0.06.

TABLE 3. Analysis of variance and multiple regression for $\Delta h_v/\gamma$, Valencia, *Universitat Politècnica de València*, 2008.

Source	GL	Sum of squares	Mean square	F-Quotient	P-Value
Model	3	9.16193	3.05398	77.71	0,0000**
Residue	12	0.471586	0.0392988	-	-
Total	15	9.63351	-	-	-
Parameter		Estimate	Standard error	T-Statistic	P-Value
Constant		-3.06916	0.420595	-7.29717	0.0000**
log (a1)		0.453908	0.0724861	6.26199	0.0000**
log (a2)		0.423399	0.0487535	8.68447	0.0000**
log (b)		-2.97115	0.281987	-10.5365	0.0000**

**Significant to 1%; R^2 adjusted from 93.88%; standard error of 0.19; mean absolute error 0.14; Durbin-Watson test of 2.25 (P=0.12); Lag_l residual autocorrelation of -0.18.

TABLE 4. Analysis of variance and multiple regression for $(P_3-P_2)/\gamma$, Valencia, *Universitat Politècnica de València*, 2008.

Source	GL	Sum of squares	Mean square	F-Quotient	P-Value
Model	3	14.5068	4.83559	74.29	0,0000**
Residue	12	0.781073	0.0650894	-	-
Total	15	15.2875	-	-	-
Parameter		Estimate	Standard error	T-Statistic	P-Value
Constant		1.67725	0.54129	3.09863	0.0092**
log (a1)		-0.144214	0.0932868	-1.54592	0.1481ns
log (a2)		-0.741803	0.0627439	-11.8227	0.0000**
log (b)		-3.65672	0.362906	-10.0762	0.0000**

**Significant to 1%; R^2 adjusted from 93.61%; standard error of 0.25; mean absolute error of 0.17; Durbin-Watson test of 1.34 (P=0.02); Lag_l residual autocorrelation of 0.23.

With the results, we can say that β and α_2 are more statistically significant than α_1, having, therefore, a greater influence on DP/γ, $\Delta h_v/\gamma$, and $(P_3-P_2)/\gamma$.

In addition, other experiments investigated the influence of geometric parameters on the hydrodynamic behavior of the Venturi injectors using CFD techniques.

Huang et al. (2009) used is the CFD method for simulating the internal flow field of Venturi injectors and the relationships between some of the structure parameters: diameter (D_2) and throat length (L_g), diameter of the top of the suction pipe (D_a), and suction capacity (q). The results showed that when the inlet pressure and the D_a position remained unchanged, q increased with the decrease in D_2 and L_g and increase in D_a. While D_a, D_2 and L_g remained unchained, the greater inlet pressure increased suction capacity.

SUN & NIU (2012), using the CFD techniques, investigated the effects of geometric parameters (relationship between throat length and diameter (λ) and between throat and nozzle diameters (β)) in the performance of a Venturi injector (average output rate, low and critical pressures, coefficient of local head loss, and fertilizer absorption ratio). The results indicated that β was the main factor in the performance of the Venturi injector, which was positively correlated with

the output rate and negatively correlated with the critical and minimum pressures, the coefficient of local head loss, and the fertilizer absorption ratio.

Figure 6 shows pressure and speed distribution in a vertically symmetrical plane in the throat for models B1, B2 and B3.

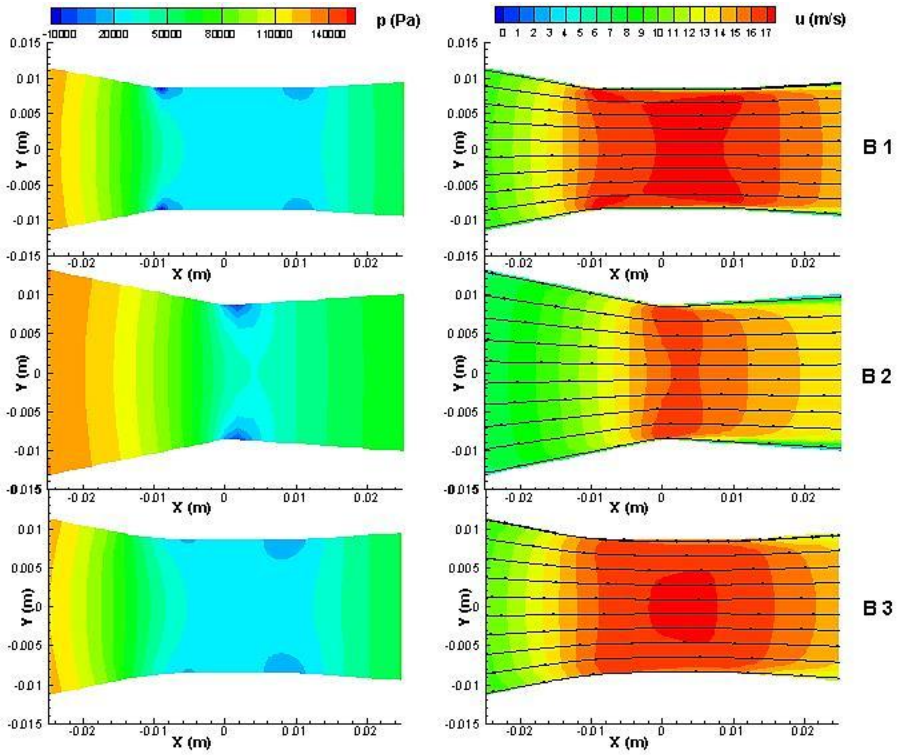

FIGURE 6. Pressure and speed distribution in the Venturi injector throat, Valencia, *Universitat Politècnica de València*, 2008. B1: nozzle-throat and throat-diffuser junctions with a sharp edge; B2: nozzle-diffuser junction with throat zero length and a sharp edge; B3: nozzle-throat and throat-diffuser junctions with a rounded edge.

In geometries B1 and B2, the minimum pressures were presented in the junction edges. In geometry B3, they were presented in the rounded joints, with higher minimum pressures.

Table 5 shows the quantitative values pressure supplied by CFD.

TABLE 5. Pressures obtained with CFD in morphologies B1, B2 and B3, Valencia, *Universitat Politècnica de València*, 2008.

Pressure (m.c.a.)	B1	B2	B3
P_1/γ	17.37	17.70	17.66
P_2/γ	2.33	4.03	2.51
P_3/γ	15.00	15.00	15.00
DP/γ	15.04	13.67	15.15
Δh_v	2.37	2.70	2.66
P_{min}/γ	-2.18	-0.23	1.84

B1: nozzle-throat and throat-diffuser junctions with a sharp edge; B2: nozzle-diffuser junction with a throat with zero length and a sharp edge; B3: nozzle-throat and throat-diffuser junctions with a sharp edge; P_1/γ: pressure at the injector outlet); P_2/γ: injector suction pressure; P_3/γ: injector output pressure; DP/γ: $P_1/\gamma - P_2/\gamma$; $\Delta h_v/\gamma$: $P_3/\gamma - P_2/\gamma$; P_{min}/γ: pressure at the lowest analyzed volume.

The head losses are similar in all three-throat geometries, while the pressure difference between the inlet and the throat is lower in geometry B2. The increased pressure in the throat, which corresponds to a lower injection flow, is given in geometry B2 while geometries B1 and B3 would be more favorable from the standpoint of the injected flow. Geometry B3 is the one that least favors the occurrence of cavitation. In summary, the rounding of the nozzle-throat and throat-diffuser junctions delays the occurrence of cavitation and reduces losses.

CONCLUSIONS

1. Based on the CFD analysis, we can conclude that the relationship of diameters is the parameter that exerts the greatest influence on the head loss in the injector. Regarding the angles, it should be pointed out that the value of the nozzle does not have a significant influence, although there is a high correlation between it and the diffuser angle.
2. The design and geometry of these devices are simple, but the geometric parameters should be controlled to achieve the best hydraulic efficiency within a specific range of operation. Thus, it will be important to select the largest possible relationship of diameters to enable the injection, and ensure that the diffuser angle is as small as possible.
3. The rounding of junctions in the morphology between nozzle-throat and throat-diffuser junctions is the most recommended one, as it reduces head losses and delays the occurrence of cavitation.

ACKNOWLEDGMENTS

The authors would like to thank the "Conselleria d'Empresa, Universitat i Ciència" of Generalitat Valenciana – Spain.

REFERENCES

AL-HASSAN, Q. An algorithm for computing inverses of tridiagonal matrices with applications. **Soochow Journal of Mathematics**, Taipei, v. 31, n. 3, p. 449-466, 2005.

ALPTEKIN, E.; EZAN, M. A.; KAYANSAYAN, N. Flow and heat transfer characteristics of an empty refrigerated container. In: ALPTEKIN, E.; EZAN, M. A.; KAYANSAYAN, N. *Progress in* **Exergy, Energy, and the Environment**. Switzerland: Springer International Publishing, 2014. p. 641-652,

ARVIZA, J. Dispositivos para fertirrigación en sistemas de riego localizado. **Vida Rural**, Lisboa, n. 123, p. 34-40, 2001.

BAYLAR, A.; AYDIN, M. C.; UNSAL, M.; OZKAN, F. Numerical modeling of Venturi flows for determining air injection rates using Fluent v. 6.2. **Mathematical and Computational Applications**, Manisa, v. 14, n. 2, p. 97-108, 2009.

CHAN, L.; CHIN, C.; SORIA, J.; OOI, A. Large eddy simulation and Reynolds-Averaged Navier-Stokes calculations of supersonic impinging jets at varying pipe-to-wall distances and impinging angles. **International Journal of Heat and Fluid Flow**, New York, v. 47, n.1, p. 31-41, 2014.

DANTAS NETO, J.; MACIEL, J. L.; ALVES, A. D. S.; AZEVEDO, C. A. de.; FERNANDES, P. D.; LIMA, V. L. de. Teores de macronutrientes em folhas de goiabeira fertirrigada com nitrogênio. **Revista Brasileira de Engenharia Agrícola e Ambiental**, Campina Grande, v. 17, n. 9, p. 962-968, 2013.

DIMITRIOS, B.; ANESTIS, K.; DIMITRIOS, S.; CHARIS-KONSTANTINA, K.; ASPASIA, E. Effects of fertilization and salinity on weed flora in common bean (*'Phaseolus vulgaris*' L.) grown following organic or conventional cultural practices. **Australian Journal of Crop Science**, Lismore, v. 8, n. 2, p. 178-182, 2014.

HUANG, X.; LI, G.; WANG, M. CFD simulation to the flow field of Venturi injector. In: LI, D.; CHUNJIANG, Z. **Computer and computing technologies in agriculture II**. Boston: Springer, 2009. p. 805-815.

ISO - INTERNATIONAL ORGANIZATION FOR STANDARDIZATION. **Measurement of fluid flow by means of pressure differential devices inserted in circular cross-section conduits running full - Part 4: Venturi tubes** *(ISO 5167-4:2003).* Genova, 2003. 34 p.

LODOÑO, C. N.; ALVAREZ, R. M.; SANTAMARIA, J. R. A. Dinámica de fluidos computacional aplicada al estudio de regeneradores térmicos. **Dyna**, Medellín, v. 71, n. 143, p. 81-93, 2004.

MANZANO, R. **Análisis del inyector Venturi y mejora de su instalación en los sistemas de riego localizado**. 2008. 248f. Tesis (Doctoral) - Departamento de Ingeniería Rural y Agroalimentaria, Universitat Politècnica de València, Valencia, 2008.

MANZANO, J.; PALAU, G. **Hydraulic modelling of Venturi injector by means of CFD**. St. Joseph: ASABE Annual International Meeting, 2005. (Paper number 052070).

MELLADO, K. L. C.; IBARRA, J. E. J.; FONSECA, F. R. F. Solución numérica de las ecuaciones de Navier-Stokes incompresibles por el método de los volúmenes finitos. **Ion**, Bucaramanga, v. 26, n. 2, p. 17-29, 2013.

REZENDE, R.; HELBEL JÚNIOR, C.; SOUZA, R. S. de.; ANTUNES, F. M.; FRIZZONE, J. A. Crescimento inicial de duas cultivares de cafeeiro em diferentes regimes hídricos e dosagens de fertirrigação. **Engenharia Agrícola**, Jaboticabal, v. 30, n. 3, p. 447-458, 2010.

SANDERS, E. B.; VAN DER PIJL, S. P.; KOREN, B. Review of computational fluid dynamics for wind turbine wake aerodynamics. **Wind Energy**, Chichester, v. 14, n. 7, p. 799-819, 2011.

SANTOS, L. da C.; ZOCOLER, J. L.; JUSTI, A. L.; SILVA, A. O.; CORREIA, J. de S. Estudo comparativo da taxa de injeção em injetor do tipo Venturi com e sem válvula de retenção. **Irriga**, Botucatu, p. 145 - 154, 2012. Edição Especial.

SUN, Y.; NIU, W. Simulating the effects of structural parameters on the hydraulic performances of Venturi tube. **Modelling and Simulation in Engineering**, Cairo, v. 1, n. 1, p. 1-7, 2012.

URIBE, R. A. M.; GAVA, G. J. de C.; SAAD, J. C. C.; KÖLLN, O. T. Ratoon sugarcane yield integrated drip-irrigation and nitrogen fertilization. **Engenharia Agrícola**, Jaboticabal, v. 33, n. 6, p. 1124-1133, 2013.

VASATA, D.; GALANTE, G.; RIZZI, R. L.; ZARA, R. A. Solução computacional do problema da cavidade cúbica através das equações de Navier-Stokes tridimensionais. **Revista Brasileira de Ensino de Física**, São Paulo, v. 33, n. 2, p. 1-10, 2011.

WENDT, J. F. **Computational fluid dynamics**: an introduction. Chaussee de Waterloo: A Von Karman Institute Book, 2009. 333 p.

YEOH, G. H.; LIU, C.; TU, J.; TIMCHENKO, V. Computational fluid dynamics and its applications. **Modelling and Simulation in Engineering**, Cairo, v. 1, n. 1, p. 1-2, 2012.